treated in hydrogen at 1073K for 30 minutes and quenched to room temperature to ensure a narrow size distribution of the silver nanoparticles. The silver nanoparticles were examined by transmission electron microscopy (TEM) [3]. The sample was used in the powdered form for PAS experiments.

The silver-polymer nanocomposite was prepared by adding a solution of Ag_2O in NH_4OH to a polyacrylamide polymer sol in distilled water and reducing the oxide to metallic silver by using formic acid [4]. The metal-polymer mixture was separated by adding ethyl alcohol, dried in an oven at 323K for 24 hours and then pressed into pellets.

For positron annihilation measurements at room temperature, a weak (~ 1.5 μCi) ^{22}Na source was either kept immersed in the volume of the powdered sample (silver-glass nanocomposite) or sandwiched between two identical pellets (silver-polymer nano composite). (In the low temperature experiments discussed later in this paper, a stronger source (~ 10 μCi) was used.) The positron lifetime measurements were carried out using a slow-fast gamma-gamma coincidence experimental set-up with a time resolution of 260 ps [5]. For Doppler broadening measurements [5] (on silver-polymer nanocomposite only), an HPGe detector with resolution 1.14 keV at 514 keV (^{85}Sr) was used.

3. Results and discussion

The positron lifetime spectra were best fitted with three exponentials (after the deconvolution of resolution and source and background correction) using the programs RESOLUTION and POSITRONFIT [6]. The values of the corresponding three lifetime components τ_i ($i = 1, 2, 3$) with relative intensities I_i ($i = 1, 2, 3$) are given in Table 1.

Table 1. Positron lifetimes and intensities and the mean silver particle size ($\bar{x}$) in the silver-glass and silver-polymer nanocomposites (M G. :- Mother glass sample (see the text), S G.N :- silver-glass nanocomposite, P P.P - pure polyacrylamide polymer sample and S.P.N. :- silver-polymer nanocomposite

Sample	τ_1 (ps)	τ_2 (ps)	τ_3 (ps)	I_1 (%)	I_2 (%)	I_3 (%)	$\bar{x}$ (nm)
M G	163 ± 2	380 ± 4	1500 ± 30	57.4 ± 1.2	41.9 ± 1.2	0.7 ± 0.1	5.0
S G.N.	155 ± 2	345 ± 4	1500 ± 30	57.3 ± 1.2	41.6 ± 1.2	1.2 ± 0.1	23.7
P P P	160 ± 6	402 ± 17	1587 ± 25	30.6 ± 2.7	47.5 ± 2.4	21.9 ± 0.4	-
S.P.N	184 ± 7	391 ± 17	1338 ± 26	37.8 ± 3.0	49.5 ± 3.1	12.7 ± 0.4	10.4

3.1 Positron lifetimes in the silver-glass nanocomposite :

Positrons emitted by the ^{22}Na source will be rapidly thermalised on entering the sample and a significant fraction of them will be captured within the nanocrystalline grains. If the grain size is less than the thermal diffusion wavelength of positrons (~ 110 nm in silver), they will diffuse out and get trapped at the grain interfaces. The origin of τ_1 in the glass and the silver-glass nanocomposite (henceforth referred simply as the "glass system") is therefore attributed to positron annihilation at the interfaces of the nanocrystalline silver grains and the glass. (The precipitation of colloidal silver in the glass, which did not undergo any reduction in hydrogen, is due to the photoreduction of silver ions for which the impurity ions in the glass act as sensitizers [7].) The second lifetime τ_2 originates from positrons trapped and annihilated at the free volume defects in the glass. Amorphous materials are characterised by a free volume

defect density which is a few orders of magnitude higher than the density of defects in crystalline solids. In the absence of the silver particles, such a high concentration of free volume defects would have led to the so-called saturation trapping where all the positrons entering the sample would have been trapped in the free volume defects. The value of 345-380 ps is typical of positrons trapped in voids of radius about 0.20 nm and each consisting of 8-10 monovacancies in crystalline solids [8]. This is also confirmed by the formation of orthopositronium atoms in large free volume defects, as indicated by the longest lifetime component τ_3. From the empirical relation given by Liu *et al* [9], the size of these defects is estimated as 0.23 nm. That the lifetime τ_1 decreases from 163 ps to 155 ps as the grain size increases from 5 nm to 23.7 nm is proof of the shrinkage of the interfacial traps with grain growth, as also pointed out in the studies by Tong *et al* recently [10].

3.2 Positron lifetimes in the silver-polymer nanocomposite :

The interpretation of the results on the polymer and the silver-polymer nanocomposite (together referred as the "polymer system") is not straightforward. In the glass system, the intensity of the orthopositronium component I_3 was such that the formation probability of parapositronium (which is one-third that of orthopositronium) was ignored. In the polymer system, however, I_3 is significantly high (12-22%) and hence the fraction $(I_3/3)\%$ of parapositronium with intrinsic lifetime 125 ps and admixed with the measured τ_1 cannot be ignored. Considering the measured value (160 ps) of τ_1 in the pure polymer as an admixture of the parapositronium lifetime and the lifetime of positrons annihilating in the bulk polymer, the latter one is estimated as 171 ps. In the silver-polymer nanocomposite, τ_1 also includes the lifetime of positrons annihilating from the defects on the grain interfaces. Extending the above argument to decompose the measured τ_1 (184 ps) into three lifetimes, the positron lifetime in the interfacial defects is estimated as 238 ps. As in the case of the glass system, the occurrence of τ_2 and τ_3 in the spectra of the polymer system could be attributed to the free volume defects and the formation of orthopositronium in large defects. The average size of the free volume defects can be estimated from the empirical relation referred earlier [9] and was obtained as 0.24 nm.

3.3. Low temperature measurements : A metal-to-semiconductorlike transition ?

The TEM observations on the silver-polymer nanocomposite gave an average particle size of 10.4 nm (Figure 1). The histogram nevertheless indicated that nanoparticles of diameter even less than 5 nm are present in significant numbers. Such a composite is an ideal system to verify the one-electron energy level splitting of metal atoms, leading to a semiconductorlike transition, as predicted by the Wood-Ashcroft theory [11]. According to this theory, the energy levels of atoms of such small particles would be discrete and the energy gap between the lowest unoccupied level and the highest occupied level would be such that a transition of the above type might be observed at a particular temperature. We tried to investigate this point by conducting Doppler broadening measurements on the spectral lineshape of positron annihilation gamma ray signals from the sample at various temperatures between 13K and 300K.

The analysis of the Doppler broadened spectral lineshape was done in terms of the S parameter, defined as the ratio of the integrated counts in a central region of around 0.6 keV on either side of the centroid to the total integrated counts under the spectrum extending from 503.3 keV to 518.7 keV. Defined as mentioned, the S parameter sensitively respond to the changes in the momentum distribution of valence electrons whereby changes in the defect properties of condensed matter can be qualitatively inferred [12]. The sample temperatures

were achieved by mounting the source-sample sandwich on to the cryotip of a Leybold refrigerator cryostat and controlling the temperature within ± 0.3 K by a LTC 60 temperature controller.

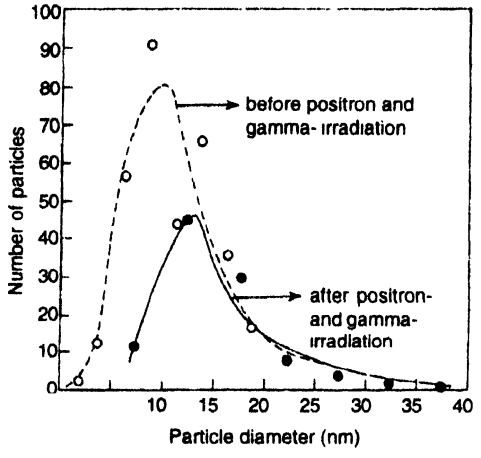

Figure 1. The size distribution of nanoparticles in the silver-polymer nanocomposite before and after the positron and gamma irradiation during the low temperature experiments.

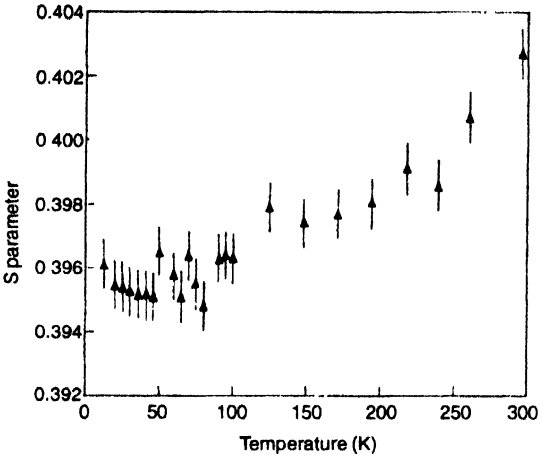

Figure 2. The variation of the S parameter *vs* temperature for the silver-polymer nanocomposite

The results of S parameter measurements *vs* temperature on the silver-polymer nanocomposite is shown in Figure 2. The overall behaviour of a decreasing trend in S with the lowering of temperature is consistent with the bulk contraction of the solid, but the anomalous features at lower temperatures need proper attention. Needless to say, the features are heavily shadowed by the effects of the polymer medium. To delineate the latter effects, identical measurements were also carried out on the pure polyacrylamide polymer sample, and the results are shown in Figure 3. Further insight into the detailed aspects of these changes was obtained by decomposing the measured S parameter (S_t) of the nanocomposite into individual

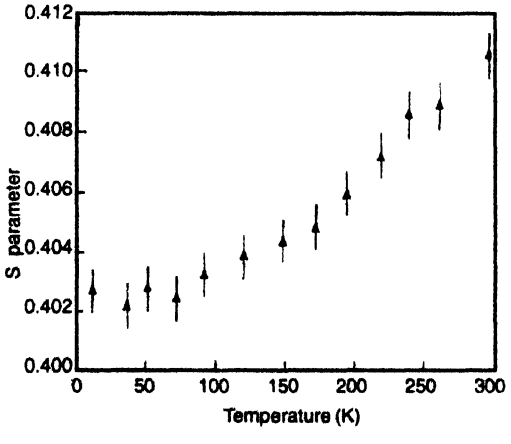

Figure 3. The variation of the S parameter *vs* temperature for the pure polyacrylamide polymer sample.

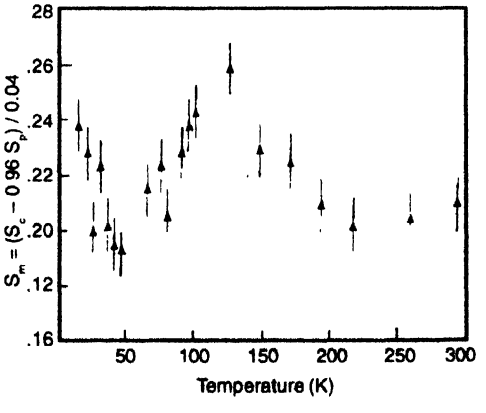

Figure 4. The computed parameter S_m *vs* temperature for the silver-polymer nanocomposite.

contributions from the pure polymer (S_p), which was measured, and the nanocrystalline metal particles (S_m) which was computed using the relation $S_c = S_m v + S_p(1-v)$. The volume fraction v of the silver nanoparticles in the nanocomposite was estimated from the densities of the composite and the polymer.

The results of this analysis is shown in Figure 4. The decreasing trend in the region 300K-210 K and 130K–45K can be accounted in terms of the lattice contraction of the particles. To explain the rises (from the direction of decreasing temperature) at 210K and 45K, we note from the work of Wood and Ashcroft [11] that the average one-electron energy level separation for a metal nanoparticle is $\Delta = E_f / N$ where E_f is the Fermi energy of the metal (5.5 eV for Ag) and N is the number of atoms in the particle. Assuming that the silver nanoparticles have got the same *fcc* structure as bulk metallic silver, where the unit cell volume a^3 on the average consists of 4 atoms, a nanoparticle of radius r will consist of $N = 16\pi r^3 / 3a^3$ atoms. Substituting these values, the size of the particles contributing to the rises at 210K and 45K are respectively found to be 2.1 nm and 3.0 nm. The histogram in Figure 1 seems to indicate the possibility of having particles of such extremely low sizes in the nanocomposite, although 2.1 nm is apparently below the resolving limit of the TEM. That the S parameter increases owing to a transition brought in by increased energy level separation further supports these arguments. Compared to a metal, a semiconductor is characterised by a larger energy level spacing. This reduces the extent of overlap of the core electron wavefunction with the wavefunction of the thermally diffusing positrons, which actually determines the annihilation probability. The positron annihilation gamma ray spectra therefore will be dominated by events due to annihilation with low momentum valence electrons [12]. The magnitude of the Doppler shift ΔE ($= p_L c/2$, where p_L is the projected electron momentum) is such that the region around the centroid will be populated in excess, resulting in a larger S by its definition.

3.4 Radiation effects on nanoparticles :

TEM observations on the silver-polymer nanocomposite after the low temperature experiments indicated the agglomeration of silver nanoparticles (Figure 1). The average particle size had increased to 14.3 nm. Positron lifetime measurements also gave indirect proof to this observation. From the results shown in Table 2 and using the scheme of analysis described in Section 3.2, the positron lifetime in the bulk polyacrylamide was obtained as 207 ps and the positron lifetime at the nanoparticle grain interfaces as 203 ps.

Table 2. Positron lifetimes and intensities in the pure polyacrylamide polymer (P P P) and the silver-polymer nanocomposite (S P.N.) after the low temperature experiments.

Sample	τ_1 (ps)	τ_2 (ps)	τ_3 (ps)	I_1 (%)	I_2 (%)	I_3 (%)
P.P.P.	190 ± 7	419 ± 23	1588 ± 36	34 8 ± 2 8	43.6 ± 3 7	21.6 ± 0.5
S P N	199 ± 6	414 ± 19	1386 ± 25	45 4 ± 3 3	43.3 ± 4.0	11.3 ± 0 3

Over a period of about 165 hours during which the low temperature experiments were carried out, the samples had been continuously bombarded by positrons (with end-point energy 0.54 MeV) and gamma rays. Considering that the source had a strength of 10 μCi, giving 3.7×10^5 positrons per second, and that each positron is associated with one 1.28 MeV and two 0.511 MeV gamma rays [12], the total energy deposited inside the samples due to the thermalization of the positrons and the attenuation of the gamma rays is estimated as 8.75 Mrad

[4, 13]. Although this energy is deposited over a long interval of time and within a volume defined by the geometrical area (~ 2 mm) of the source and the range of penetration of the positrons in the sample (~ 0.8 mm for 0.54 MeV), it could lead to the breaking of the polymer chains and hence additional free space would become available for the trapping of positrons. This explains the increase in the positron lifetime in the polymer bulk from 171 ps before the low temperature experiment to 207 ps after it. The additional free space also favours the agglomeration of the silver nanoparticles, leading to an increase in the average particle size. As already mentioned earlier, the increase in the particle size would lead to a decrease in the lifetime of the positrons trapped and annihilated at the grain interfaces [4]. We observe that the positron lifetime has indeed fallen from 238 ps before the low temperature experiment to 203 ps after it.

4. Conclusions

We have shown in this work that the structural properties of nanocrystalline grain interfaces can be studied from the annihilation characteristics of positrons diffusing out to the grain surfaces. The synthesis of isolated nanoparticles in a glass or polymer medium is found equally successful like the metal evaporation and condensation technique in this investigation. We observed a shrinkage of the interfacial defect volume with increasing grain size, resulting in a decrease in positron lifetime. The investigation at low temperatures also gave evidence to a metal-to-semiconductorlike transition. The positron and gamma irradiation effects lead to particle agglomeration, resulting in a reduced positron lifetime at the interfaces after the low temperature experiments.

Acknowledgments

This work was done at SINP in collaboration with Dr. M. Mukherjee and Prof. D. Chakravorty of the Indian Association for the Cultivation of Science, Calcutta. Their collaboration was supported by a foreign research grant No. N00014-93-1-0040 of the Office of Naval Research, Virginia, U.S.A. The author is grateful to Prof. Prasanta Sen for moral support and constant encouragement.

References

[1] R Birringer, H Gleiter, H -P Klein and P Marquardt *Phys. Lett* **102A** 365 (1984)

[2] H -E Schaefer, R Wurschum, R Birringer and H Gleiter *Phys. Rev.* **B38** 9545 (1988)

[3] M Mukherjee P M G Nambissan and D Chakravorty *J. Phys. : Condens. Matter* **8** 5649 (1996)

[4] M Mukherjee, D Chakravorty and P M G Nambissan *Phys. Rev.* **B57** 848 (1998)

[5] P M G Nambissan and P Sen *Philos. Mag.* **A62** 173 (1990)

[6] P Kirkegaard, M Eldrup, O E Mogensen and N J Pedersen *Comput. Phys. Commun.* **23** 307 (1981)

[7] P W McMillan in *Glass Ceramics* (London : Academic) (1964)

[8] M J Puska and R M Nieminen *J. Phys.* **F13** 333 (1983)

[9] J Liu, Q Deng and Y C Jean *Macromolecules* **26** 7149 (1993)

[10] H Y Tong, B Z Ding, J T Wang, K Lu, J Jiang and J Zhu *J. Appl. Phys.* **72** 5124 (1992)

[11] D M Wood and N W Ashcroft *Phys. Rev.* **B25** 6255 (1982)

[12] R W Siegel, *Annu. Rev. Mater. Sci.* **10** 393 (1980)

[13] Takenori Suzuki, Taichi Miura, Yuichi Oki, Masaharu Numajiri, Kenjiro Kondo and Yasuo Ito *Radiat. Phys. Chem.* **45** 657 (1995)